

Design of a global extremum seeking algorithm for an omni-directional robot model

E. Dincmen

*Işık University, 34980, Şile, İstanbul, Turkey
(Tel: 0090-2165287127; e-mail: erkin.dincmen@isikun.edu.tr).*

Abstract: A global extremum seeking algorithm is developed for a mobile robot model where the aim is to find the location of the most powerful signal source among the others. In other words, the control problem is to seek the global extremum point of a performance function when there are local extremas. The locations of the signal sources and signal distribution characteristics are unknown, i.e. the gradient of the performance function is unknown. The control algorithm also doesn't use any position measurement of the mobile robot itself. Henceforth, the controller is suitable for the missions where the robot moves in an unknown terrain with no GPS signal and no inertial measurements. Only the signal magnitude should be measured via a sensor mounted on the robot during the motion. A gradient estimator is designed to determine the motion direction towards the extremum point. When a local extremum is found, the robot will continue its search for another extremum points. Once each extremums have been visited, the robot will compare the signal levels on each source and identify the global extremum i.e. the most powerful signal source. In the absence of any position measurements, the robot can move towards the global extremum by repeating its motion history backwards. In the literature, this is the first global extremum seeking algorithm that has been developed for an omni-directional mobile robot model. Via the simulation studies it has been shown that the control algorithm can seek and find both stationary and non stationary signal sources and it can find the global extremum point when there are local extremas.

Keywords: Global optimization, extremum seeking, omni-directional robot, gradient estimation.

1. INTRODUCTION

The mainstream methodology in control applications is to regulate considered plant to known set points. However, in some control problems, the relation between the set point and desired system performance is unknown. One situation is that, the performance function of the system reflecting the desired system behavior has an extremum value and the control objective is to seek a priori unknown optimum operation point. This problem can be solved via the extremum seeking algorithm, which is suitable for the problems that possess completely or partially unknown performance functions and these functions may also change in time.

In the literature, extremum seeking schemes are divided into four main groups which are perturbation based, sliding mode based, numerical optimization based and gradient based methods. In the perturbation based extremum seeking algorithms (Bratcu et al., 2008; Ghaffari et al., 2014; Krstic and Wang, 2000; Zhang et al., 2007a; Zhang et al., 2007b), disturb and observe methodology is conducted by adding a perturbation to the search signal. According to the result of the perturbation on the system output, increment or decrement action for the search signal is determined. In Dincmen et al., 2014; Dincmen and Guvenc, 2012; Drakunov et al., 1995; Fu and Ozguner, 2011; Haskara et al., 2000, sliding mode techniques are utilized for seeking the extrema of the unknown functions. A sliding surface is designed such that on sliding mode, the system output should approach

towards the optimum operation point. The numerical optimization based extremum seeking schemes (Vweza et al., 2015; Zhang and Ordonez, 2007) use various iteration algorithms to find the optimum operation point. The iteration method finds the target state and a state regulator manage the system follow this new state. In Guay and Dochain, 2015; Guay, 2014, extremum seeking is accomplished via adaptive gradient estimation techniques.

In this paper, a new global extremum seeking algorithm is developed for an omni-directional mobile robot model where the aim is to find the most powerful signal source among the other sources in the operation region of the robot. Mobile robots have taken enormous attention in recent years for various application areas such as cleaning, surveillance, transportation, agriculture, manufacturing, military applications, medical/surgical applications etc. In Rossomando et al., 2014, sliding mode control method is proposed for a nonholonomic mobile robot using adaptive neural network. Penizzotto et al., 2014 aims to provide a metric for human inattention in teleoperation of mobile robots. In Santhanakrishnan et al., 2016, an experimental implementation of the morphological transform is presented to extract the features of the environment of the mobile robots. In Ilas et al., 2011, a group of algorithms for determining the possible trajectories of mobile robots while navigating through obstacles have been presented. Majdik et al., 2011 presents a visual mapping system for a security robot application.

Among the mobile robot types, omni-directional mobile robots (Barreto et al., 2014; Kim and Kim, 2014; Li et al., 2015; Taheri et al., 2012) have wheels with free rollers which results a holonomic constraint.

The research objective of this paper is to develop a control algorithm for omni-directional mobile robots, whose missions are searching the locations of signal sources without using any GPS or inertial measurements. Hence, the developed controller is suitable for robots operating in unknown terrains where no GPS and no inertial measurements are available. Possible practical implementation examples of the proposed controller could be as follows: By using a gas or chemical agent detection sensor, searching the sources of gas or chemical leaks in underground facilities, tunnels. By using radiation detectors, searching the sources of radiation leakages in nuclear reactors. Space mining applications such as mine searching in planets and asteroids. Military applications such as by using thermal sensors, locating hostile forces or terrorists in underground bunkers and caves.

The developed control algorithm doesn't know the locations of the signal sources and the distribution characteristics of the signals. In other words, gradients of the performance function are unknown. Also, position measurement of the mobile robot itself is not necessary. Only the magnitude of the signal should be measured via a sensor mounted on the robot during the motion. It is assumed that the signal magnitudes are decreasing away from the sources.

The methodology of the control algorithm is estimating the gradients of the signal distribution function, i.e. the performance function via the sliding mode technique. The motion direction of the mobile robot is determined via a gradient climbing rule based on these gradient estimations. Once an extremum point has been found, the robot will continue its search towards the other extremas. After finding all extremum points, the robot will determine the global extremum i.e. the most powerful signal source by comparing the signal levels among the extremum points. Without having any position measurement device, the robot can move towards the global extremum point by repeating its motion history backwards.

The key features of the proposed control algorithm are summarized as follows: Firstly, without knowing the signal distribution function and the location of the extremum points, and without using a GPS signal or inertial measurements, the robot can find the global extremum point i.e. the most powerful signal source among the other signal sources i.e. local extremas.

Secondly, in the gradient climbing mode, the motion of the robot is determined based on the gradient estimations. For these gradient estimations, the discontinuous functions u_1 and u_2 that will be introduced in Section 3 are used. Although discontinuous functions are used for gradient estimation, they are not used directly as control inputs. Rather than that, their values are low-passed, which means that the high frequency oscillations in u_1 and u_2 do not appear in the control inputs.

Thirdly, according to the gradient climbing rule that will be introduced in Section 3, the control inputs will oscillate only around the extremum points since the sign of the gradients changes only around the peak points. This will cause no problem because once the robot reaches an extremum point, it will leave this point and begin a new search towards finding other extremas.

This is the first approach in the literature that a global extremum seeking algorithm is developed for an omni-directional mobile robot model.

Via the simulation studies it has been shown that the control algorithm can seek and find both stationary and non stationary signal sources and it can find the global extremum point when there are local extremas. The rest of the paper is organized as follows: In Section 2, omni-directional mobile robot model is introduced. The control algorithm is presented in Section 3. Simulation studies are given in Section 4. The paper ends with conclusions in Section 5.

2. MOBILE ROBOT MODEL

A three-wheeled omni-directional mobile robot model is considered in this paper. Each wheel has free rollers which results a holonomic robot. In Fig. 1, schematic representation of the robot is shown. Here, V_{w1} , V_{w2} and V_{w3} are the translational velocities of the wheels. Longitudinal velocity of the robot in x axis is denoted as u , lateral velocity in y axis is v and r is the rotational velocity of the robot around its center i.e. the z axis. Robot radius is denoted as R .

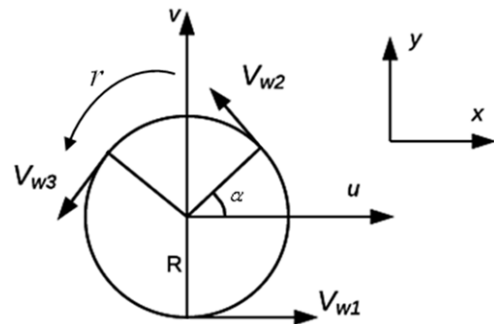


Fig. 1. Three wheeled omni-directional mobile robot model.

Translational velocities of the wheels can be calculated from the rotational velocities as $V_{wi} = R_w \omega_i$ ($i=1,2,3$), where R_w is the wheel radius and ω_i are the angular velocities of the wheels. The kinematic equations of the robot can be written as

$$V_{w1} = R_w \omega_1 = u + Rr, \quad (1)$$

$$V_{w2} = R_w \omega_2 = -u \sin(\alpha) + v \cos(\alpha) + Rr, \quad (2)$$

$$V_{w3} = R_w \omega_3 = -u \sin(\alpha) - v \cos(\alpha) + Rr. \quad (3)$$

3. CONTROL ALGORITHM

The change of the signal distribution with respect to the inertial coordinates (x,y) is denoted here as a performance function $J(x,y)$, which has multiple extremum points. In other words, the aim is to find the most powerful signal source among the other sources. The signal distribution function, i.e. $J(x,y)$ is unknown but only the magnitude of the signal can be

measured via a sensor mounted on the robot during the motion. The controller doesn't know the location of the extremum points, i.e. the signal sources. Additionally, the position measurement of the robot is not available. At the first stage of the controller design, the sliding surface is selected as

$$s = J(x, y) + z_1 + z_2, \quad (4)$$

where the time derivatives of the variables z_1 and z_2 are defined as

$$\dot{z}_1 = -\dot{x}u_1, \quad (5)$$

$$\dot{z}_2 = -\dot{y}u_2. \quad (6)$$

In (5) and (6), u_1 and u_2 are discontinuous functions of the sliding variable s given as

$$u_1 = M_1 \operatorname{sgn} \left[\sin \left(\frac{\pi s}{\gamma_1} \right) \right], \quad (7)$$

$$u_2 = M_2 \operatorname{sgn} \left[\sin \left(\frac{\pi s}{\gamma_2} \right) \right], \quad (8)$$

where $M_1, M_2, \gamma_1, \gamma_2$ are positive constants, "sgn" is the signum function and "sin" is the sinusoidal function. By taking the time derivative of (4), one can obtain the equality

$$\dot{s} = \frac{\partial J}{\partial x} \dot{x} + \frac{\partial J}{\partial y} \dot{y} - \dot{x}u_1 - \dot{y}u_2. \quad (9)$$

3.1 Necessary Condition to Make $\dot{s} = 0$ during Motion on x Axis

For a time interval Δt , when only motion on x axis is allowed, then, since $\dot{y} = 0$ during this interval, the equation given in (9) becomes

$$\dot{s} = \frac{\partial J}{\partial x} \dot{x} - \dot{x}u_1. \quad (10)$$

Theorem: If M_1 in (7) is chosen to satisfy the condition

$$M_1 > \left| \frac{\partial J}{\partial x} \right|_{\max}, \quad (11)$$

then, after a finite time interval, the time derivative of s in (10) will be equal to $\dot{s} = 0$.

Proof: From (10) and (7), one can obtain

$$\dot{s} = \frac{\partial J}{\partial x} \dot{x} - \dot{x}M_1 \operatorname{sgn} \left[\sin \left(\frac{\pi s}{\gamma_1} \right) \right]. \quad (12)$$

By denoting the velocity of the mobile robot on x axis as a positive constant, e.g. $\dot{x} = V$, then, one can write (12) as

$$\dot{s} = \frac{\partial J}{\partial x} V - VM_1 \operatorname{sgn} \left[\sin \left(\frac{\pi s}{\gamma_1} \right) \right]. \quad (13)$$

Assuming that the initial value of the sliding surface variable s is between the constant values of $\gamma_1 < s(0) < 2\gamma_1$. Then, the following mathematical equality can be written for s values on that interval,

$$\operatorname{sgn} \left[\sin \left(\frac{\pi s}{\gamma_1} \right) \right] = \operatorname{sgn}(s - 2\gamma_1). \quad (14)$$

Equation (14) can be justified from Fig. 2. It is realized that when the value of the sliding surface variable s is between $\gamma_1 < s(0) < 2\gamma_1$, then the value of the function $\operatorname{sgn}[\sin(\pi s / \gamma_1)]$ is equal to -1 and the value of the function $\operatorname{sgn}(s - 2\gamma_1)$ is also equal to -1.

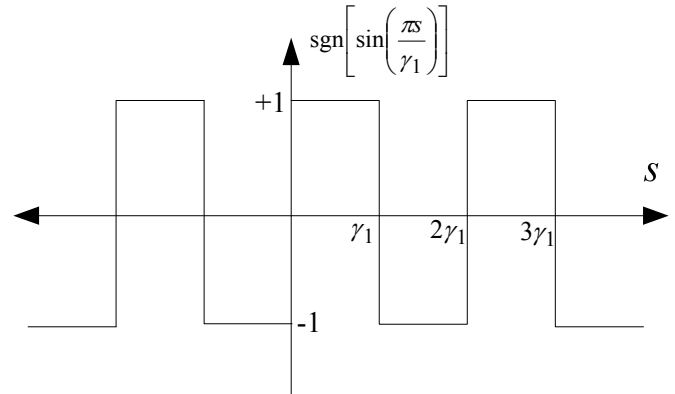


Fig. 2. Function of $\operatorname{sgn}[\sin(\pi s / \gamma_1)]$.

Then, (13) can be written as

$$\dot{s} = \frac{\partial J}{\partial x} V - VM_1 \operatorname{sgn}(s - 2\gamma_1). \quad (15)$$

Now, by defining a variable λ as

$$\lambda = s - 2\gamma_1, \quad (16)$$

and since $\dot{\lambda} = \dot{s}$, one can write from (15) following equation

$$\dot{\lambda} = \frac{\partial J}{\partial x} V - VM_1 \operatorname{sgn}(\lambda). \quad (17)$$

By multiplying (17) with λ , one can obtain

$$\lambda \dot{\lambda} = \frac{\partial J}{\partial x} V \lambda - VM_1 |\lambda|. \quad (18)$$

From (18), following inequality can be written

$$\lambda \dot{\lambda} \leq \left| \frac{\partial J}{\partial x} \right| V |\lambda| - VM_1 |\lambda| = -V |\lambda| \left(M_1 - \left| \frac{\partial J}{\partial x} \right| \right). \quad (19)$$

So, in (19), when M_1 is chosen to satisfy the condition (11), the absolute value of λ will decrease and approach to zero in finite time because (19) is the finite time stability condition. After the finite time, since $\lambda = 0$ will be true, one can write from (16)

$$s = 2\gamma_1; \dot{s} = 0, \quad (20)$$

which means that $\dot{s} = 0$ is achieved. It should be noted that the condition in (11) means that the value of the M_1 parameter should be larger than the maximum value of the performance function gradient with respect to x . Although the gradient is unknown since $J(x, y)$ function is unknown, still one can anticipate the maximum possible gradient value and choose an M_1 value which will always satisfy the condition (11).

The above analysis was conducted for the case where the mobile robot moves in positive x direction with a speed of $\dot{x} = V$. On the contrary, when the robot moves in negative x direction, i.e. when $\dot{x} = -V$, then (12) can be written as

$$\dot{s} = -\frac{\partial J}{\partial x}V + VM_1 \operatorname{sgn}\left[\sin\left(\frac{\pi s}{\gamma_1}\right)\right]. \quad (21)$$

Again, if the initial value of s is between $\gamma_1 < s(0) < 2\gamma_1$, then, similar to (14), the following mathematical equality can be also written on that interval

$$\operatorname{sgn}\left[\sin\left(\frac{\pi s}{\gamma_1}\right)\right] = -\operatorname{sgn}(s - \gamma_1). \quad (22)$$

Equation (22) can be justified again via the help of Fig. 2. So, (21) becomes

$$\dot{s} = -\frac{\partial J}{\partial x}V - VM_1 \operatorname{sgn}(s - \gamma_1). \quad (23)$$

This time, if the variable λ is defined as

$$\lambda = s - \gamma_1, \quad (24)$$

since $\dot{\lambda} = \dot{s}$, one can write from (23)

$$\dot{\lambda} = -\frac{\partial J}{\partial x}V - VM_1 \operatorname{sgn}(\lambda). \quad (25)$$

By multiplying (25) with λ , one can obtain

$$\lambda \dot{\lambda} = -\frac{\partial J}{\partial x}V\lambda - VM_1|\lambda|. \quad (26)$$

From (26) the following inequality can be written

$$\lambda \dot{\lambda} \leq \left|\frac{\partial J}{\partial x}\right|V|\lambda| - VM_1|\lambda| = -V|\lambda|\left(M_1 - \left|\frac{\partial J}{\partial x}\right|\right). \quad (27)$$

In the above inequality, by choosing M_1 to satisfy the condition (11), the absolute value of λ will decrease and after a finite time, $\lambda = 0$ will be true. Then from (24) one can write

$$s = \gamma_1; \dot{s} = 0, \quad (28)$$

which shows that again $\dot{s} = 0$ is achieved. So, whether $\dot{x} = V$ or $\dot{x} = -V$, by choosing u_1 as in (7) and assuring the condition (11), $\dot{s} = 0$ can be achieved after a finite time interval. *End of proof*

The above analysis was conducted when the initial value of s is between the constant values $\gamma_1 < s(0) < 2\gamma_1$. It can be easily shown that the above proof can be repeated for any initial value of $s(0)$. So, whatever the initial value of s is, after a finite time interval $\dot{s} = 0$ will be achieved.

3.2 Gradient Estimation during Motion on x Axis

When $\dot{s} = 0$ is accomplished in (10), and when the motion on x axis is maintained at all times during Δt , i.e. $\dot{x} \neq 0$, then, from (10), the equivalent value of the discontinuous function u_1 will be equal to

$$u_{1eq} = \left(\frac{\partial J}{\partial x}\right)_{est}. \quad (29)$$

In other words, gradient estimation of the performance function with respect to x can be accomplished by calculating the equivalent value of the discontinuous function u_1 given in (7). To obtain the equivalent value of the discontinuous function u_1 , a low pass filter can be used as

$$\left(\frac{\partial J}{\partial x}\right)_{est} = u_{1eq} = \frac{1}{\tau_1 p + 1} u_1, \quad (30)$$

where τ_1 is the filter time constant and p is the Laplace operator. So, in (30), $1/(\tau_1 p + 1)$ is the transfer function of a first order system, which is the low-pass filter here. The rationale for using a low-pass filter to obtain the equivalent value of the discontinuous function u_1 can be explained as follows: Since u_1 is a discontinuous function given in (7), when $\dot{s} = 0$, then the values of u_1 will oscillate with high frequency. Mean value (equivalent value) of these oscillations can be derived by filtering out the high frequency component with using a low-pass filter. So, the gradient of the performance function with respect to x will be estimated as u_{1eq} from (30). It should be reminded that the performance function $J(x, y)$, i.e. the signal distribution function is unknown. Henceforth, the exact gradient value $\partial J/\partial x$ is unknown. The controller will use only the estimated gradient value $(\partial J/\partial x)_{est}$ which is calculated from (30).

3.3 Gradient Climbing Rule during Motion on x Axis

Desired velocity set value during motion on x axis can be calculated by using the estimated gradient from (30) according to the following gradient climbing rule,

$$\dot{x}_{set} = V_1 \operatorname{sgn}^*\left(\left(\frac{\partial J}{\partial x}\right)_{est}\right) = V_1 \operatorname{sgn}^*(u_{1eq}), \quad (31)$$

where V_1 is a positive constant and representing the step size of the gradient climbing. The function sgn^* is defined as

$$\operatorname{sgn}^*(\alpha) = \begin{cases} 1 & \text{if } \alpha \geq 0 \\ -1 & \text{otherwise} \end{cases}. \quad (32)$$

According to (31) and (32), the velocity set points on x axis will take values $\dot{x}_{set} = \pm V_1$.

3.4 Necessary Condition to Make $\dot{s} = 0$ during Motion on y Axis

After Δt interval, motion on x axis will be stopped and the robot will start to move on y axis for another Δt time interval. So, since $\dot{x} = 0$ will be true during motion on y axis, the equation given in (9) becomes

$$\dot{s} = \frac{\partial J}{\partial y} \dot{y} - \dot{y} u_2. \quad (33)$$

During motion on y axis, it will be true that $\dot{y} \neq 0$. If M_2 in (8) is selected to satisfy the inequality

$$M_2 > \left|\frac{\partial J}{\partial y}\right|_{\max}, \quad (34)$$

then, after a finite time, the time derivative of s will be equal to $\dot{s} = 0$. The proof of this section will be similar to the proof given in Section 3.1, hence it is not repeated here. It should be reminded that although the gradient with respect to y is unknown, one can anticipate the maximum value of the gradient and choose the M_2 constant which will always satisfy the condition (34).

3.5 Gradient Estimation during Motion on y Axis

If $\dot{s} = 0$ is accomplished in (33), then the equivalent value of the discontinuous function u_2 will be equal to

$$u_{2eq} = \left(\frac{\partial J}{\partial y} \right)_{est}, \quad (35)$$

which is the estimate of the performance function gradient with respect to y . To obtain the equivalent value of the discontinuous function u_2 , a low pass filter similar to (30) can be used as

$$\left(\frac{\partial J}{\partial y} \right)_{est} = u_{2eq} = \frac{1}{\tau_2 p + 1} u_2, \quad (36)$$

where τ_2 is the time constant of the second filter.

3.6 Gradient Climbing Rule during Motion on y Axis

Desired velocity value on y axis can be calculated by using the estimated gradient value u_{2eq} from (36) according to the following gradient climbing rule,

$$\dot{y}_{set} = V_2 \operatorname{sgn}^* \left(\frac{\partial J}{\partial y} \right)_{est} = V_2 \operatorname{sgn}^* (u_{2eq}), \quad (37)$$

where V_2 is a positive constant and the function sgn^* is defined previously in (32). So, the velocity set point on y axis will take values $\dot{y}_{set} = \pm V_2$.

3.7 Overall Gradient Climbing Controller

The controller scheme of the gradient climbing rule is shown in Fig. 3. As mentioned before, the performance function $J(x,y)$, i.e. the signal distribution characteristics is unknown and the position measurement of the robot itself is not used in the control structure. The only input to the controller is the signal amplitude J obtained from a sensor during the motion of the robot. Since u_1 and u_2 are discontinuous functions of s , their values will oscillate with high frequencies when $\dot{s} = 0$. However, the values of u_1 and u_2 are not directly used as control inputs. Their values are passed through the low pass filters as shown in (30), (36). The filtered values of u_1 and u_2 are the estimated gradient values. Control inputs are calculated by using these estimated gradient values. Hence, the high frequency oscillations in u_1 and u_2 will not enter directly as the control input.

After calculating longitudinal and lateral set point velocities from (31) and (37), the desired wheel angular velocities can be calculated by using kinematic equations of the mobile robot given in (1), (2) and (3) as follows,

$$\begin{bmatrix} \omega_{1set} \\ \omega_{2set} \\ \omega_{3set} \end{bmatrix} = \frac{1}{R_w} \begin{bmatrix} 1 & 0 & R \\ -\sin(\alpha) & \cos(\alpha) & R \\ -\sin(\alpha) & -\cos(\alpha) & R \end{bmatrix} \begin{bmatrix} \dot{x}_{set} \\ \dot{y}_{set} \\ r_{set} \end{bmatrix}. \quad (38)$$

In this paper, it is assumed that the mobile robot doesn't rotate around its axis, i.e. $r_{set} = 0$. Once the setpoint wheel angular velocities ω_{1set} , ω_{2set} and ω_{3set} are calculated from (38), the velocity controller will control the wheel motors to track these wheel set velocities. This paper doesn't include a velocity controller and perfect tracking of the set velocities is assumed. For the velocity controller, a well known PID controller can be used.

3.8 Searching the Global Extremum Point

When an extremum point is found, the robot will leave this point and continue its search for other extremas. Eventually, after visiting all extremums, the robot can determine the global extremum by comparing the signal magnitude levels on the visited extremum points. In the absence of any position measurement, the robot can move towards the global extremum point by repeating its motion history backwards.

Two different operation modes are defined here for the mobile robot. In the "Gradient Climbing Mode", the motion of the robot is determined via the gradient climbing controller shown in Fig. 3. In this mode, the robot moves towards an extremum point via the rules of (31) and (37). Once an extremum is found, "Gradient Climbing Mode" is deactivated and "Single Move Mode" will be activated. In this second mode, the robot will move away from the extremum point and step into a neighborhood. Then, "Gradient Climbing Mode" will be activated again to initiate a new search towards the next extremum point. The shape of the performance function and the location of the extremum points are unknown. However, the number of extremum points, i.e. the number of signal sources should be known in advance in order the robot not to continue its search forever. The graphical representation of the global search algorithm in one dimension is shown in Fig. 4. The block diagram of the robot operation modes are given in Fig. 5. Switch block shown in Fig. 5 is used to change the operation modes. When the robot reaches an extremum point, i.e. Region 2 in Fig. 4, the change of the signal magnitude becomes very small. Then, the switch will activate the "Single Move Mode", where the robot will move linearly for a predefined amount of time in order to leave the previous extremum point and start a new search. Flow diagram of the robot operation is shown in Fig. 6.

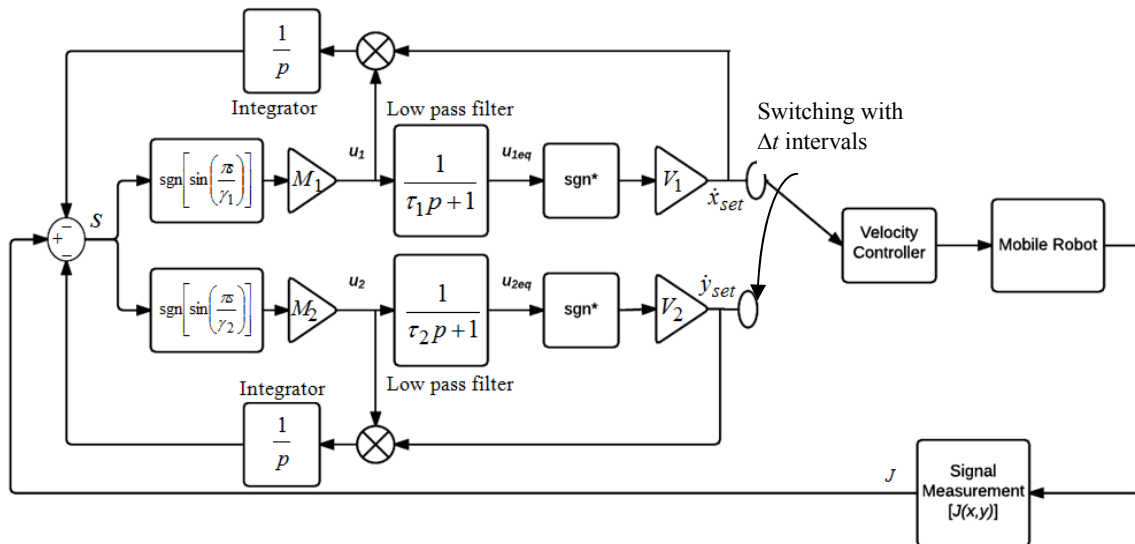


Fig. 3. Gradient climbing controller.

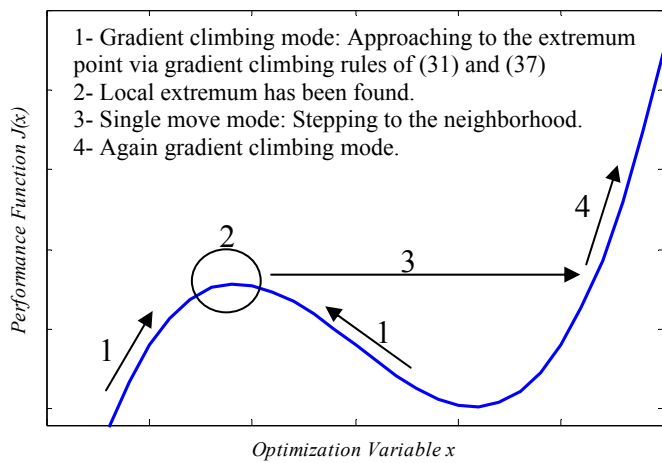


Fig. 4. Schematic representation of the global extremum seeking in one dimension.

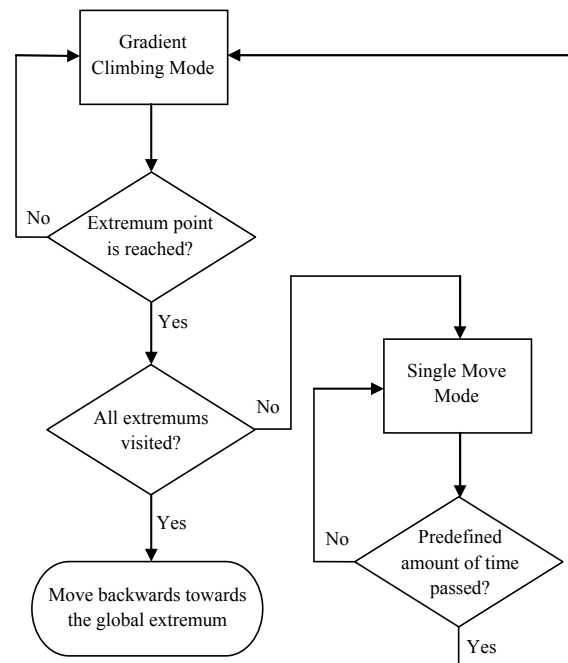


Fig. 6. Flow diagram of the robot operation.

4. SIMULATION STUDIES

The performance of the control algorithm is evaluated via simulation studies. The Matlab/Simulink model used in the simulations is shown in Fig. 7. The detail of the “GradientClimbingMode” block is shown in Fig. 8. Here, pulse generator blocks generate 0 and 1 values with specified intervals so that they provide stair shaped move of the robot during gradient climbing mode. In other words, during gradient climbing, the robot will move for a predefined amount of time on x axis, then for a predefined amount of time on y axis and then again on x axis etc. The details of the “GradientClimbing_x” and “GradientClimbing_y” blocks are shown in Fig. 9 and Fig. 10, respectively. They generate set velocities on x and y axes according to (31) and (37) during gradient climbing.

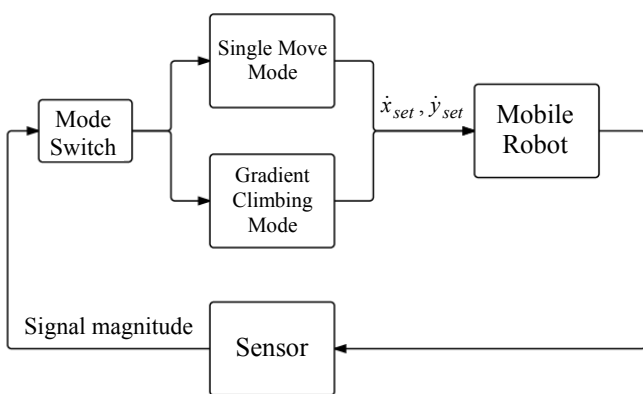


Fig. 5. Robot operation modes.

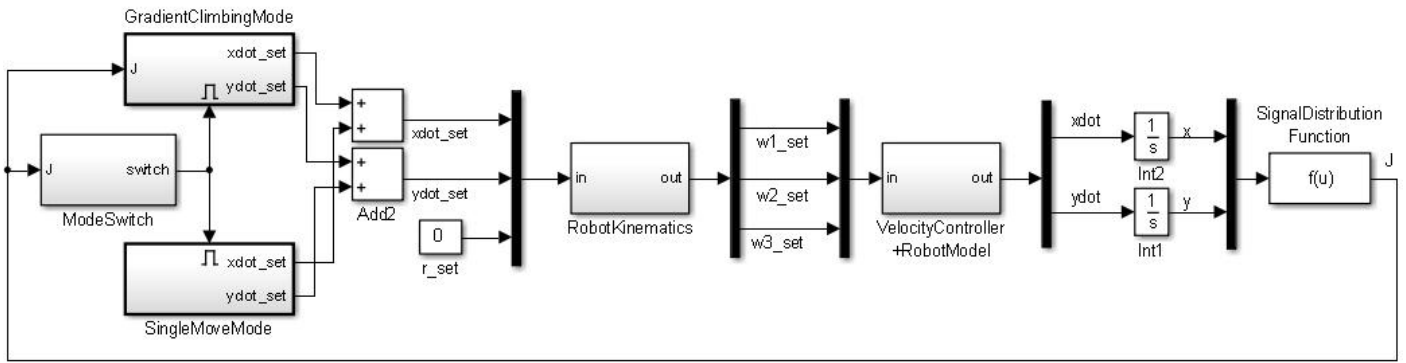


Fig. 7. Simulink model used in the simulations.

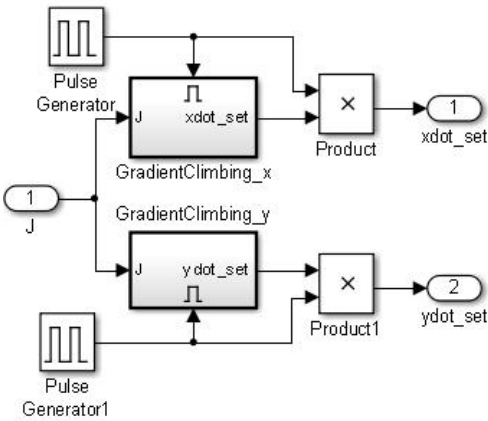


Fig. 8. Block diagram of the “GradientClimbingMode” subsystem.

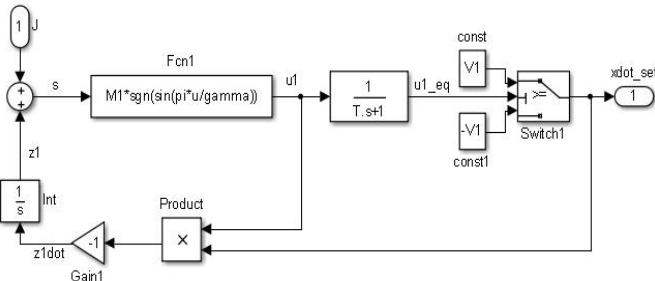


Fig. 9. Block diagram of the “GradientClimbing_x” subsystem.

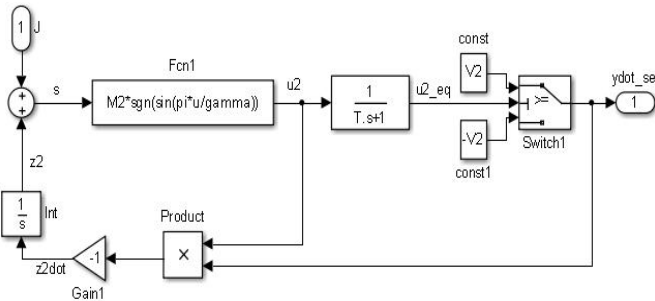


Fig. 10. Block diagram of the “GradientClimbing_y” subsystem.

Simulation studies are divided into four cases. In the first scenario, the performance function has one extremum point, i.e. there is one signal source in the operation region of the robot. Via this simulation, the gradient climbing performance

is evaluated by plotting robot trajectory and control inputs (wheel set point velocities). In the second simulation scenario, the moving signal source case is studied and it is shown that the robot can find and track the moving signal source. In the third simulation scenario, the performance function has two extremum points. It is shown that the robot is able to find the global extremum point when there are local extremas. In the fourth simulation scenario, the effect of the step size magnitude value on the gradient climbing performance is investigated. Lastly, the simulation results are compared with an existing implementation in the literature.

4.1 Single Extremum Case

For the first simulation study, the signal distribution is simulated via the function

$$J(x, y) = 1 - 0.5x^2 - 0.25y^2 \tag{39}$$

Signal distribution function (39) is plotted in Fig. 11. The function obtains its maximum value $J_{max}=1$ at $x_{opt}=0, y_{opt}=0$. As introduced before, the controller doesn't know the function (39) and the x_{opt}, y_{opt} values. Also the position of the robot is not measured. Only, the magnitude of the signal should be obtained via a sensor mounted on the robot during the motion.

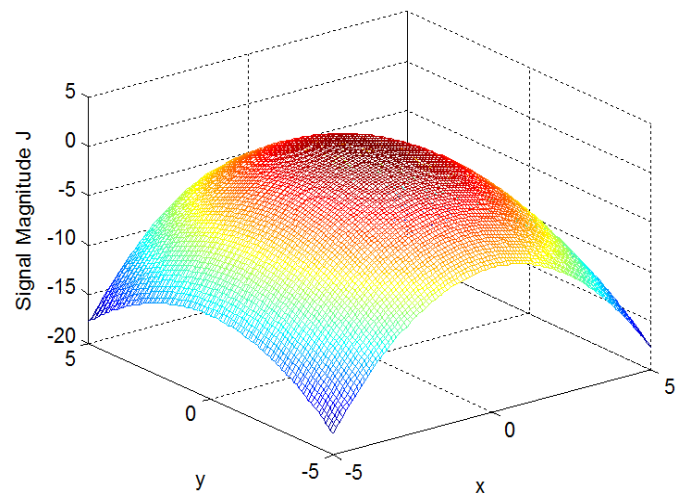


Fig. 11. Signal distribution function given in (39).

The initial position of the robot is chosen as $x(0)=3, y(0)=3$. In Fig. 12, change of the robot trajectory via gradient climbing controller is plotted. It is realized that starting from

the point (3, 3), the robot moves towards the extremum point (0, 0). During the motion of the robot, the change of the signal magnitude J is plotted in Fig. 13. As shown, after approx. 11 sec., the robot finds the optimum point where the signal magnitude obtains its maximum value. The reference wheel angular velocities which are calculated from (38) are shown in Fig. 14. In the gradient climbing mode, the motion of the robot is determined via the estimation of the gradients as given in (31) and (37). Since the sign of the gradient of a function will change only around the peak points, the control inputs will oscillate only around the extremum points. As shown in Fig. 14, the calculated wheel reference velocities start to oscillate when the robot reaches the peak point, which occurs after 11 sec. The oscillations point out that the robot has found the signal source.

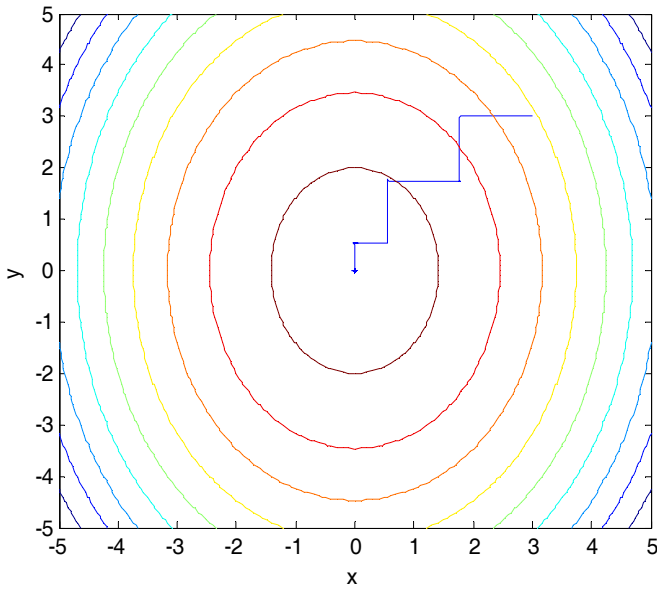


Fig. 12. The trajectory of the mobile robot for single extremum case.

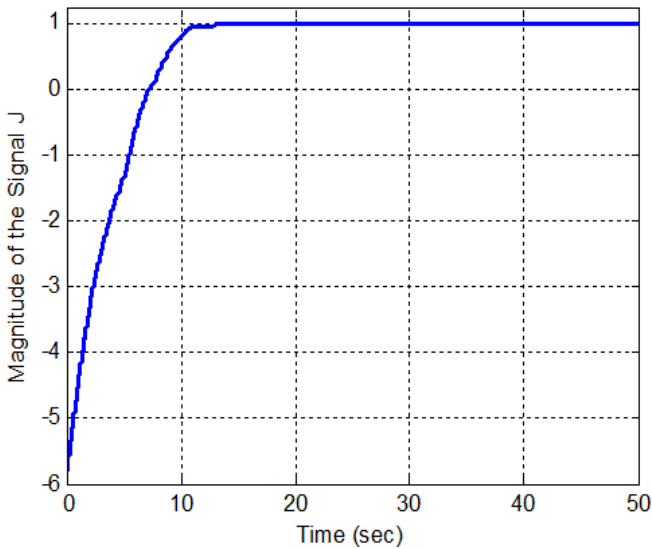


Fig. 13. Change of the signal magnitude with respect to time during the motion of the robot.

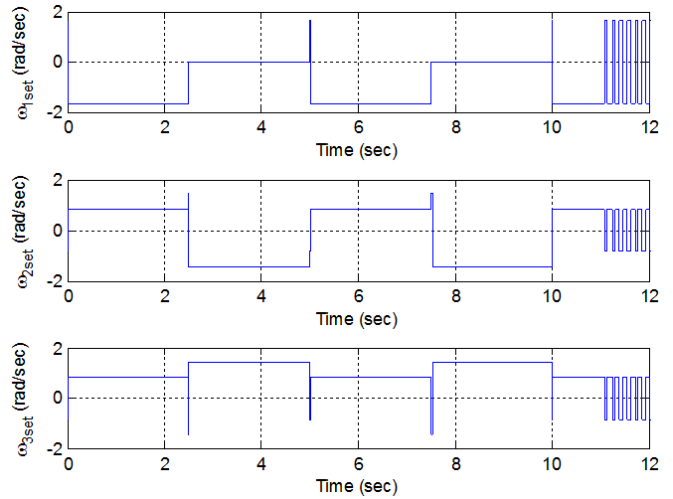


Fig. 14. Change of the control inputs with respect to time.

In the simulations, the value of Δt is chosen as 2.5 sec. It means that the robot starts its motion on x axis and it moves on this axis for 2.5 sec. Afterwards, it starts to move on y axis for another 2.5 sec. Then again on x axis for 2.5 sec and this stair shaped move as shown in Fig. 12 continues until the robot finds the extremum point, i.e. the signal source.

4.2 Moving Signal Source Case

In the above study, the signal source was stationary. Next, the simulation is conducted for a moving signal source case. For this second simulation study, the signal distribution function is simulated via the following time dependent function (Zhang et al., 2007a)

$$J(x, y) = 1 - 0.5[x - \sin(0.03t)]^2 - 0.25[y - \sin(0.06t)]^2 \quad (40)$$

In Fig. 15, the signal source and robot trajectories are plotted. It is shown that the mobile robot finds and tracks the moving target. The change of the signal magnitude during the tracking phase is plotted in Fig.16, where it is realized that the robot manages perfect tracking of the moving target.

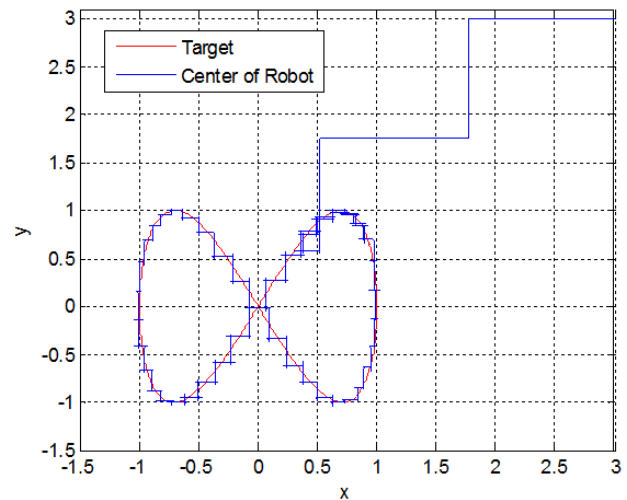


Fig. 15. Change of the signal source and mobile robot trajectories for moving target case.

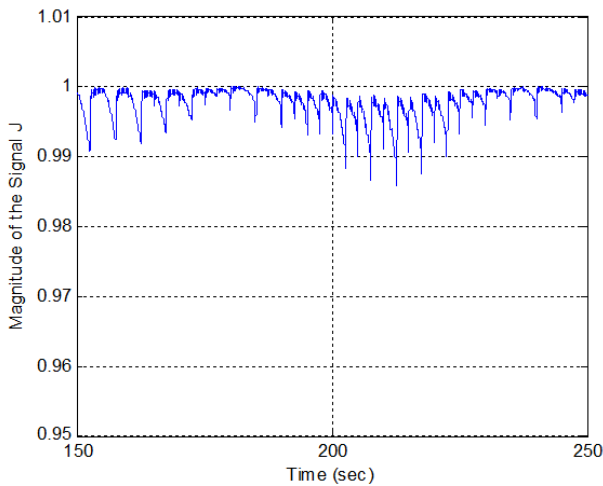


Fig. 16. Change of the signal magnitude with respect to time during moving target tracking.

4.3 Multiple Extremum Case

In the third simulation scenario, finding the global extremum point when there are local extremas cases is studied. The signal distribution characteristic is simulated here via the following performance function (Matveev et al., 2011),

$$J(x, y) = 10e^{-\frac{(x-10)^2 + (y-8)^2}{600}} + 18e^{-\frac{(x+20)^2 + (y+12)^2}{200}} \quad (41)$$

The plot of the performance function is shown in Fig. 17. The signal distribution function has two extremum values. In Fig. 18, the robot trajectory during the simulation is shown. The initial point of the robot was chosen again as $x(0)=3, y(0)=3$. Firstly, the robot approaches to the local extremum point of the region via the gradient climbing rules (31) and (37). It should be noted that although the gradient climbing rules includes sign terms, the control inputs will oscillate only when the robot reaches to an extremum point because the gradient of a function will change its sign only around the extremum points. This will cause no problem because once the robot reaches an extremum point; it will leave this point and begin a new search towards the other extremas.

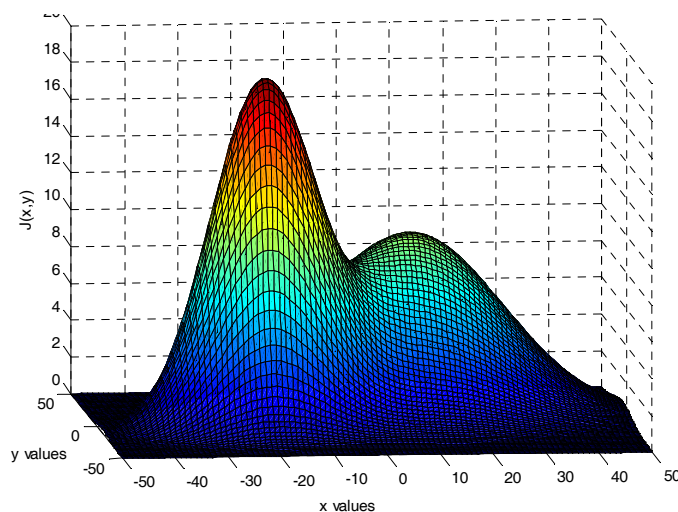


Fig. 17. Signal distribution function given in (41).

As shown from Fig. 18, once the first extremum point is found, “Gradient Climbing Mode” is deactivated and “Single Move Mode” is activated where the robot moves linearly for a predefined amount of time in order to reach to a different region. Then, again via the “Gradient Climbing Mode”, the robot reaches extremum point of this new region. The flow diagram of the robot operation was given before in Fig. 6. Since the second extremum point is the global extremum, control algorithm stopped and the robot remained on this point.

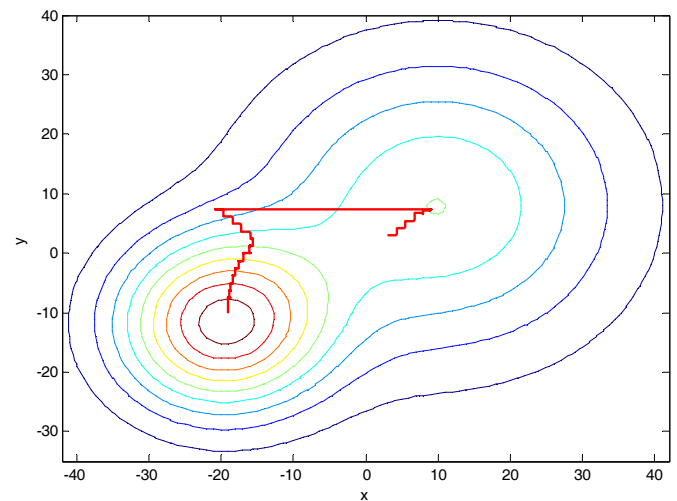


Fig. 18. The trajectory of the mobile robot for multiple extremum case.

4.4 Effect of the Step Size Magnitude in Gradient Climbing Performance

In the gradient climbing mode, the robot moves towards the extremum point i.e. the signal source via the rules given in (31) and (37). In these equations, V_1 and V_2 determine the step sizes in the gradient climbing phase on x and y axes. In order to examine the effect of the step size magnitude value on the gradient climbing performance of the mobile robot, the simulation study shown in Section 4.1 is repeated with three different step size values. The step size magnitudes are taken equal during motions on x and y axes i.e. $V_1=V_2$. Fig. 19 shows changes of the signal values and Fig. 20 shows the trajectories of the robots.

From Fig. 19, it is realized that increment of the step size magnitude improves gradient climbing time. When the step size is chosen as $V_1 = V_2 = 1$, the robot finds the signal source in approx. 7 sec. For the step size of 0.5, the duration becomes approx. 11 sec and for the step size of 0.1, it will be approx. 60 sec. Hence, the magnitude of the step size has a major effect on the performance of the algorithm.

It should be noted that increment of the step size may result the robot miss some extremum points, i.e. signal sources. If the signal sources are located close to each other, in other words if one extremum point is near to its neighbour extremum point, then a big step size may result the robot pass by one extremum point and approach to the other one. Hence, the step size of the robot should be selected such that while the robot is able to visit all extremum points, at the same time it can find the extremum points in a shorter time.

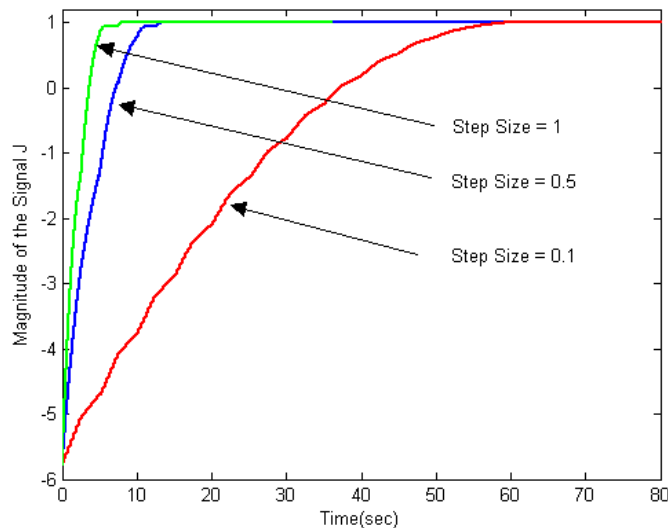


Fig. 19. Change of the signal values during gradient climbing with different step sizes.

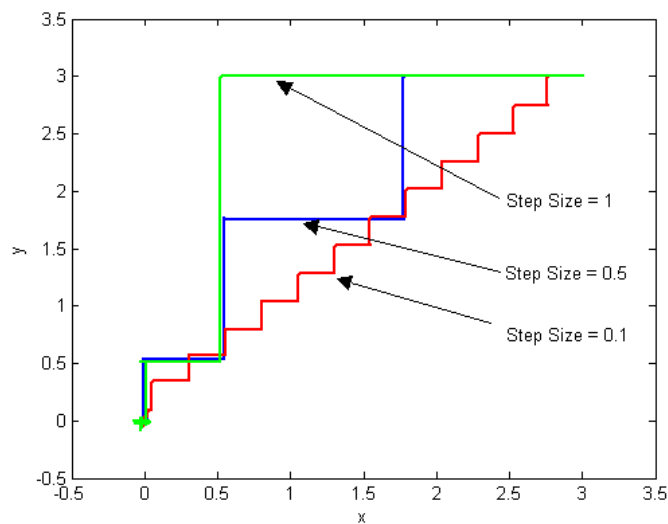


Fig. 20. Trajectories of the mobile robot during gradient climbing with different step sizes

4.5 Comparison of the Results with Existing Implementations

In Zhang et al., 2007b, extremum seeking algorithm was used for an autonomous vehicle. A velocity actuated point mass was considered as the vehicle model, which has motion characteristics similar to the omni-directional mobile robot model considered here. Perturbation based extremum seeking algorithm was utilized as the source seeking controller. Both stationary and moving signal source case was studied. In this methodology, periodic perturbations such as $asin\omega t$ were added to the control inputs of the autonomous vehicle. The perturbation $asin\omega t$ created periodic response in the motion output of the robot, which is either in phase or out of phase with $asin\omega t$. When input and output sinusoids are in phase, it means that the vehicle is moving in positive gradient region of the signal distribution function (in case of a concave function) and when they are out of phase, it is understood that the vehicle is moving in negative gradient region. By using filters, this information was deduced and motion direction of the vehicle was determined. Since this algorithm used

sinusoidal perturbations, the motion of the autonomous vehicle showed circular trajectories as shown in Fig. 4b and Fig. 5b in Krstic et al., 2007b. The control inputs had continuous oscillations during the entire motion of the robot as shown in Fig. 4c, Fig. 4d, Fig. 5c and Fig. 5d (Krstic et al., 2007b). On the other hand, in the proposed control algorithm here, the robot shows straight trajectories during motions on x and y axes, as shown in Fig. 12, Fig. 15 and Fig. 18. The control inputs are constant during motions on x axis and y axis as shown in Fig. 14. The control inputs start to oscillate only when the robot finds the extremum point. Henceforth, the proposed control methodology here is advantageous because of less aggressive control effort.

5. CONCLUSION

Unlike classical regulative control schemes, extremum seeking covers control problems where the operation point for optimum system performance is unknown and it is searched online. In this paper, a new global extremum seeking method is proposed for the source seeking controller of an omni-directional mobile robot model. The key features of the proposed controller are summarized as follows: Without knowing the signal distribution function and the location of the extremum points, and without using a GPS signal and inertial measurements, the robot can find the global extremum point i.e. the most powerful signal source among the other local extremas. Hence, the developed controller is suitable for robots operating in unknown terrains with no GPS and inertial measurements. Only the signal magnitude should be measured via a sensor mounted on the robot during its motion. In the gradient climbing mode, the motion of the robot is determined via the estimation of the gradient of the performance function. For the gradient estimation, the functions u_1 and u_2 given in (7) and (8) are used. Since u_1 and u_2 are discontinuous functions of s , their values will oscillate with high frequencies when $\dot{s}=0$. However, the values of u_1 and u_2 are not directly used as control inputs. Their values are passed through low pass filters. Hence, the high frequency oscillations in u_1 and u_2 will not enter directly to the control inputs. Since the gradient of a function changes its sign only around the peak points, the control inputs calculated from (31) and (37) will oscillate only around the extremum points. This will cause no problem because once the robot reaches an extremum point; it will leave this point and begin a new search towards the other extremas. Finally, after visiting all extremas, the robot will move towards the global extremum point by repeating its motion history backwards. This is the first global extremum seeking algorithm in the literature that has been developed for an omni-directional mobile robot model. Via the simulation studies it has been shown that the control algorithm can seek and find both stationary and non stationary signal sources and it can find the global extremum point when there are local extremas.

REFERENCES

- Barreto, C. L., Conceicao, A. G. S., Dorea, C.E.T., Martinez, L., Roberto de Pieri, E. (2014). Design and implementation of model-predictive control with friction compensation on an omnidirectional mobile robot.

- IEEE/ASME Transactions on Mechatronics*, 19 (2), 467-476.
- Bratcu, A.I., Munteanu, I., Bacha, S., Raison, B. (2008). Maximum power point tracking of grid-connected photovoltaic arrays by using extremum seeking control. *Journal of Control Engineering and Applied Informatics*, 10 (4), 3-12
- Dincmen, E., Guvenc, B.A., Acarman, T. (2014). Extremum seeking control of ABS braking in road vehicles with lateral force improvement. *IEEE Transactions on Control Systems Technology*, 22 (1), 230-237.
- Dincmen, E., Guvenc, B. A. (2012). A control strategy for parallel hybrid electric vehicles based on extremum seeking. *Vehicle System Dynamics*, 50 (2), 199-227.
- Drakunov, S., Özgüner, Ü., Dix, P., Ashrafi, B. (1995). ABS control using optimum search via sliding modes. *IEEE Transactions on Control Systems Technology*, 3 (1), 79-85.
- Fu, L., Özgüner, Ü. (2011). Extremum seeking with sliding mode gradient estimation and asymptotic regulation for a class of nonlinear systems. *Automatica*, 47, 2595-2603.
- Ghaffari, A., Krstic, M., Seshagiri, S. (2014). Power optimization and control in wind energy conversion systems using extremum seeking. *IEEE Transactions on Control Systems Technology*, 22 (5), 684-1695.
- Guay, M., Dochain, D. (2015). A multi-objective extremum-seeking controller design technique. *International Journal of Control*, 88 (1), 38-53.
- Guay, M. (2014). A time-varying extremum-seeking control approach for discrete-time systems. *Journal of Process Control*, 24 (3), 98-112.
- Haskara, I., Ozguner, U., Winkelman, J. (2000). Extremum control for optimal operating point determination and set point optimization via sliding modes. *Journal of Dynamic Systems, Measurement, and Control*, 122 (4), 719-724.
- Ilas, C., Novischi, D., Paturca, S., Ilas, M. (2011). Real-time image processing algorithms for object and distances identification in mobile robot trajectory planning. *Journal of Control Engineering and Applied Informatics*, 13 (2), 32-37.
- Kim, H., Kim, B.K. (2014). Online minimum-energy trajectory planning and control on a straight-line path for three-wheeled omnidirectional mobile robots. *IEEE Transactions on Industrial Electronics*, 61 (9), 4771-4779.
- Krstic, M., Wang, H.H. (2000). Stability of extremum seeking feedback for general nonlinear dynamic systems. *Automatica*, 36 (4), 595-601.
- Li, X., Zhao, G., Jia, S., Xu, C., Qin, B. (2015). Velocity measurement for omni-directional intelligent wheelchair. *Transactions of the Institute of Measurement and Control*, doi: 10.1177/0142331215587041
- Majdik, A. L., Szoke, I., Popa, M., Tamas, L., Lazea, G. (2011). Mapping techniques for AMPLE, an autonomous security mobile robot. *Journal of Control Engineering and Applied Informatics*, 13 (1), 18-24.
- Matveev, A.S., Teimoori, H., Savkin, A.V. (2011). Navigation of a unicycle-like mobile robot for environmental extremum seeking. *Automatica*, 47 (1), 85-91.
- Penizzotto, F., Slawinski, E., Mut, V. (2014). Method to estimate human inattention in teleoperation of mobile robots. *Journal of Control Engineering and Applied Informatics*, 16 (3), 94-105.
- Rossomando, F. G., Soria, C., Carelli, R. (2014). Sliding mode control for trajectory tracking of a non-holonomic mobile robot using adaptive neural networks. *Journal of Control Engineering and Applied Informatics*, 16 (1), 12-21.
- Santhanakrishnan, M. N., Rayappan, J. B. B., Kannan, R. (2016). poXNOR morphological transform based feature extraction for mobile robot applications. *Journal of Control Engineering and Applied Informatics*, 18 (1), 42-50.
- Taheri, M., Dehkordi, M.N., Sharafi, M., Nadimi, M. (2012). Control and analysis of an omnidirectional autonomous robot based on software approach and multimedia database. *Journal of Control Engineering and Applied Informatics*, 14 (2), 65-72.
- Utkin, V., Guldner J., Shi, J. (2009). *Sliding mode control in electromechanical systems*, CRC Press.
- Vweza, A.O., Chong, K. T., Lee, D. J. (2015). Gradient-free numerical optimization-based extremum seeking control for multiagent systems. *International Journal of Control, Automation and Systems*, 13 (4), 877-886.
- Zhang, C., Arnold, D., Ghods, N., Siranosian, A., Krstic, M. (2007a). Source seeking with non-holonomic unicycle without position measurement and with tuning of forward velocity. *Systems and Control Letters*, 56, 245-252.
- Zhang, C., Ordóñez, R. (2007). Numerical optimization-based extremum seeking control with application to ABS design. *IEEE Transactions on Automatic Control*, 52 (3), 454-467.
- Zhang, C., Siranosian, A., Krstic, M. (2007b). Extremum seeking for moderately unstable systems and for autonomous vehicle target tracking without position measurements. *Automatica*, 43, 1832-1839.